RESISTIVITY LOWS NEAR PAEROA FAULT (TVZ, NZ) CAUSED BY TOPOGRAPHIC EFFECTS

G. F. RISK AND H.M BIBBY

IGNS, Wellington, NZ

ABSTRACT - Modelling of two-dimensional resistivity structures has been undertaken using a finite elements scheme that allows for accurate matching of the elevation of the ground surface. With this modelling program, interpretations were made of apparent resistivities measured with the multiple-source bipoledipole array along several lines crossing the northern part of the Paeroa Fault. On a line crossing the Paeroa Scarp near its highest point, where the throw is 425 m, the topographic effect is inferred to cause the apparent resistivities to be lowered by about 40 %, which accounts for the measured resistivity anomaly at the fault scarp. At the north-west of the Waikite-Puakohurea thermal region on another line, the topographic effect of a 100 m high ridge on Mt Waikorapa causes the apparent resistivities to be reduced by about 15 %. This is insufficient to explain the measured low-resistivity anomaly. Thus, low-resistivity rock is inferred to underlie the site, suggesting that the thermal region extends about 1 km further to the north-westward than previously thought.

INTRODUCTION

Multiple-source bipole-dipole resistivity measurements, made in 1993 along several lines crossing the northern part of the Paeroa Fault, yielded several resistivity lows near the fault. The interpretation of these data by Risk *et* al. (1994) showed that some of these low resistivity values are related to the Waikite thermal region, but others occurred at points of high elevation along the crest of the Paeroa Range and on a rhyolite ridge forming the south-westem part of Mt Waikorapa (Fig. 1). This suggests that the low apparent resistivities may have been caused by topographic disturbances. Because the computer modelling program used by Risk *et* al. (1994) assumed a flat earth, the extent of any such topographic disturbances could not be investigated.

The work reported in this paper falls into two parts. Firstly, the computer program for modelling the resistivity data was modified to allow for two-dimensional variations of surface topography. This has proved satisfactory for modelling the data in question, since the Paeroa Scarp, the ridge on Mt Waikorapa, and several other land features of the region have predominantly two-dimensional topography (Fig. 1). The second part of the work has been to use the computer program to model and interpret the data along the four lines shown in Fig. 1, with the aim of assessing the magnitude of the topographic effects and determining which of the resistivity lows are caused by hydrothermal activity.

PREVIOUS RESISTIVITY AND RELATED SURVEYS

As well as the multiple-source bipole-dipole resistivity survey of Risk *et* al. (1994), other resistivity measurements in the vicinity of the Paeroa Fault include Schlumberger array surveys which have been presented in map form by Geophysics Division (1985) and Bibby *et al.* (1993). Bibby *et al.* (1994) present an updated map of the Schlumberger array AB/2 = 500 m resistivity data which is shown here as Fig. 2. They also give an analysis of these data in the Waimangu, Waiotapu-Waikite, and Reporoa regions. Bromley (1993, 1994) made a controlled-source audio-frequency magnetotelluric resistivity survey of a small area at the foot of the Paeroa scarp between Waikite and Te Kopia.

Recent summaries of the geology of the region have been given by Wood (1994) and Grindley *et* al. (1994), while Glover et al. (1992) and Stewart (1994) have investigated the chemistry of the Waikite springs. Bibby *et al.* (1995) give an assessment of heat output from Waikite.

COMPUTER MODELLING METHODS

The computer modelling of resistivity structures undertaken in this work used a two-dimensional finite element technique, based on the work of Coggon (1971). With a two-dimensional distribution of resistivity, the potential produced by a set of current sources can be represented numerically as a Fourier transform along the strike direction (y), reducing the problem to one of determining a solution in the x-z plane. This solution is obtained using a finite element system in which the x-z plane is subdivided into a network of triangular elements each with constant resistivity. The potential (transform) is determined at each of the vertices (nodes) of the triangular elements. An example of part of the network used for the model along line D'D" is shown in Fig. 3. At each node on the surface where an apparent resistivity is to be calculated, the Fourier transform is inverted to give the potential and its gradient along strike. From this gradient and the gradient perpendicular to strike, the apparent resistivity is calculated. It was found that greater accuracy can be achieved by using a residual potential for the finite element calculations. This is done by subtracting, from the full solution, the potential that would be obtained with the same current sources in a uniform half-space. This removes the numerical singularities caused by the current sources and improves the stability of the calculations. Tests of this modelling method suggest that, under most circumstances,

the derived apparent resistivity values are accurate to within **2%.**

The advantage of the finite element method lies in the flexibility afforded by the triangular element network which can be set up to give smoothly dipping interfaces between regions of differing resistivity. The resistivities of the regions and the locations of the interfaces can be easily adjusted.

Because we are using the singularity removal process **as** part of the finite element calculations, the uppermost row of nodes of the finite element network must be flat, which does not allow undulating topography. We have overcome this limitation **by** adjusting the elevations of the line of nodes immediately below the surface to match the surface topography (Fig. 2). Above this line, the elements of the surface layer are given a high resistivity value to represent air. This method **was** found to provide satisfactory numerical stability.

MULTIPLE-SOURCE BIPOLE DIPOLE METHOD

With the multiple-source bipole-dipole method, current is injected sequentially into each of three current bipoles with different orientations. At field stations in the survey region, measurements of the resulting electric field strengths for each of the current bipoles can be analysed to give total field apparent resistivities and the corresponding directions of the electric field vectors. However, in order to remove the influences of the current bipole orientations on the apparent resistivity values, it is better to present these data in the form of a 4-element apparent resistivity tensor (eg. Bibby, 1977, **1986).** These tensors can be represented in a number of forms, each of which can be used to highlight certain features of the ground structure. In particular, the rotational invariants of the tensor ***(P_1, P_2,*** Bibby **1986)** are very useful since they can be thought of as average values of the ground resistivity, independent of orientation of the source field. Alternatively, the tensor can be represented graphically **as** an ellipse for which the length of the diameter in a particular direction is proportional to the apparent resistivity that would be measured when the electric field is aligned in that direction.

Of the possible forms, Bibby **(1986)** showed that the P_1 invariant gives the best representation of the resistivity distribution beneath the measurement sites, even for quite complex three-dimensional bodies. In this paper, we will use P_1 for the modelling process.

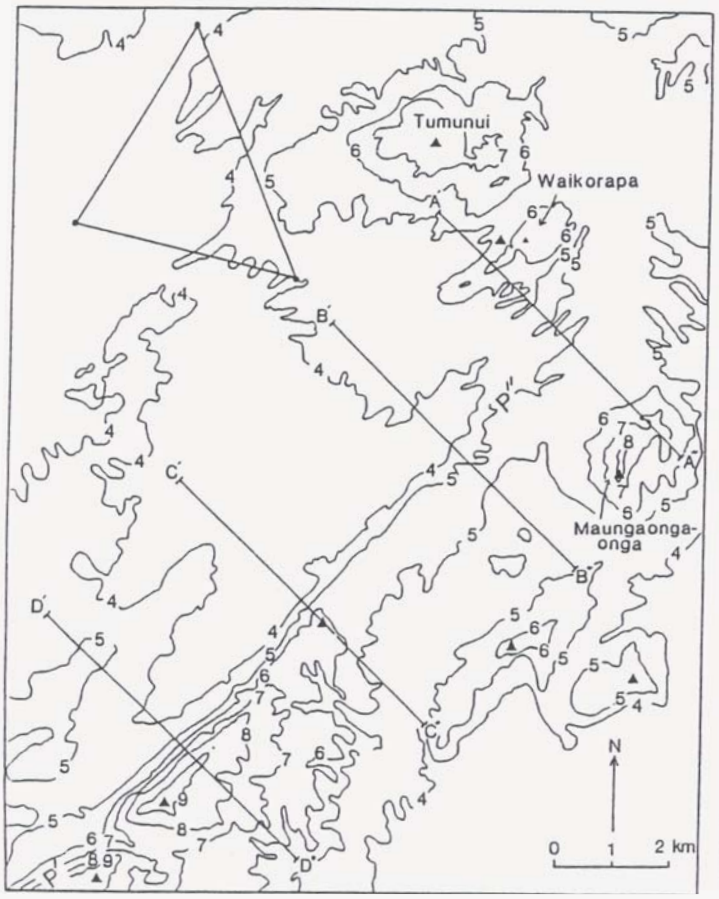

Fig. 1: Map of region around northern part of Paeroa Fault showing contours of surface topography (in units of 100 m). P'P" indicates the Paeroa Fault. A'A", B'B", C'C' and D'D" are the lines of the sections. Triangles show topographic highs. Dots denote current electrodes for the multiple-source bipole-dipole survey.

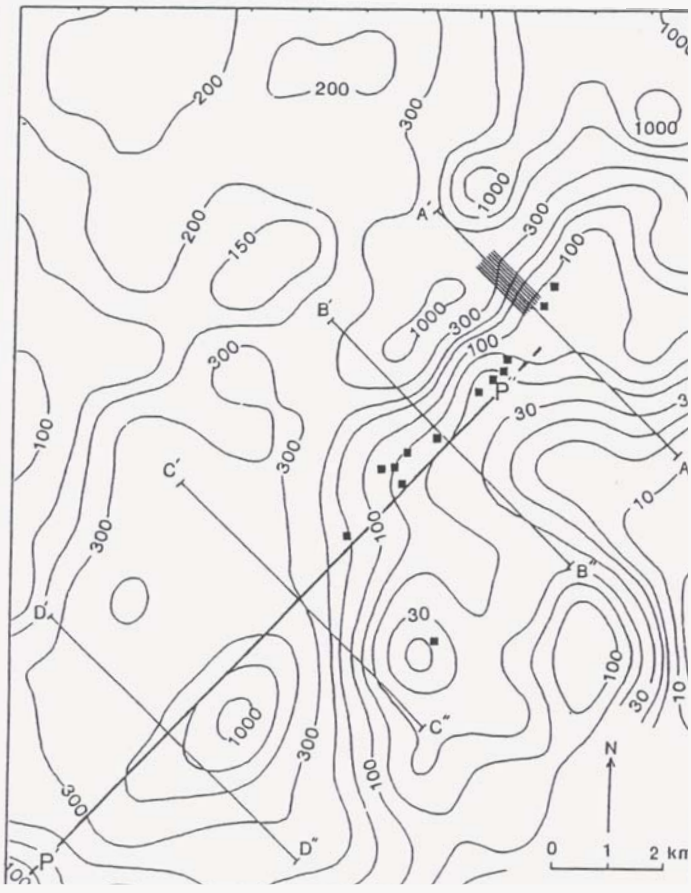

Fig. 2: Apparent resistivities (in Ωm) measured with Schlumberger array of electrode spacing AB/2 = 500 m (from Bibby et al., 1994). Line P'P" is the Paeroa Fault Shaded area on line A'A" denotes the westward extension to the low-resistivity region inferred from this work Squares at Waikite indicate thermal features.

MODELLING WITH UNIFORM EARTH

Investigation of the magnitude the topographic effects with the multiple-source bipole-dipole array was first done using a model of a uniform earth (resistivity 100 Ωm) with the surface topography found on line D'D". Since this line crosses the Paeroa Fault near the point of greatest throw, it provides an example of very large variation in two-dimensional topography (Fig. 4a). On the western side, the scarp rises by over 400 m over a horizontal distance of only about 500 m, an average slope of more than 35°. The crest is a narrow ridge less than 100 m wide and, to the east, the slope drops away at about 8°. Since the model earth has a uniform resistivity of 100 Rm, the magnitude of effect of topography on the apparent resistivities can be gauged by how much they deviate from 100 Rm.

Theoretical apparent resistivities (Fig. 4b) were first calculated using a model with a hypothetical current source about 6 km west of the scarp. The measurement points lay on a traverse line running through the current source and oriented perpendicular to the scarp. This arrangement allows apparent resistivities for individual current bipoles oriented parallel (polar) and perpendicular (equatorial) to the traverse line to be calculated, as well as the tensor components. With the transmitter aligned in the polar position, for which current flows perpendicularly across the scarp, a striking apparent resistivity low with a minimum value of 34 Rm is obtained (Fig. 4b). Placing the transmitter in the equatorial position, which causes the current to flow parallel to the scarp, produces no significant resistivity anomaly. The P_2 apparent resistivities gives a sharp anomaly of similar shape to the polar one, but with a minimum of 58 Rm. Fig. 4b also shows other small anomalies corresponding to changes of slope. In particular, apparent resistivity highs occur at the break in slope at the base of the scarp and at the lowest point in the valley, and a resistivity low occurs over the two-dimension ridge about 2.5 km west of the Paeroa Fault.

Further modelling runs were made with the transmitting array offset from line D'D" by 6.9 km to the north, which corresponds to the arrangement of current electrodes used with the field measurements. The P_2 apparent resistivities (shown in Fig. 4c) give a curve almost the same as that obtained with the transmitter on line D'D' (Fig. 4b). The minimum value is 59 Ωm (*i.e.*, a reduction of 41 %..

For complex resistivity structures, the magnitude of a topographic resistivity anomaly will depend also on the actual distribution of resistivities in the vicinity of the topographic feature. However, a simple first-order topographic correction can be made by assuming a uniform earth and multiplying the observed apparent resistivities by the factors indicated in Fig. 4. For example, at the crest of the Paeroa Scarp the P_2 value from the model (Fig. 4c) is reduced to 59 percent of the underlying resistivity. This suggests that, for line D'D", the measured P_2 of 38 Rm should be corrected to 64 Rm, which would bring it more into agreement with the values obtained at adjacent measurement points. However, because this type of correction is only approximate, it is better to combine the topographical correction process with the process of modelling the earth as a series block structures with different resistivities.

MODELLING TWO-DIMENSIONAL STRUCTURES

Line A: Line A'A" (Figs. 1, 2 & 5) crosses a 100 m high two-dimensional ridge on the southern side of Mt. Waikorapa, passes across the northern reaches of the Paeroa Fault Zone and then crosses the northern slopes of Mt Maungaongaonga to end near Waiotapu. Attention was drawn by Risk e?*al.* (1994) to a measurement at the crest of the Waikorapa Ridge of a low P_2 apparent resistivity of 32 Rm, significantly smaller than values of 120 Ωm and 55 Rm measured at adjacent sites. Risk e?*al.* (1994) could not determine whether the low value was caused by thermal ground at the site or by a topographic effect, although modelling by Fox et *al.* (1980) indicated that topographic highs could cause such a resistivity low. After entering a detailed description of the topography along line A'A' into the new computer modelling program, it was shown that the topographic effect of the ridge emplaced in a uniform earth causes apparent resistivities to be lowered by about 15 % below the resistivity of the earth (Fig. 5a). Correcting the measured value by this amount gives 38 Rm, which is still smaller than the adjacent resistivity values. We, therefore, conclude that the ground at the site is indeed conductive.

Two-dimensional resistivity models along A'A' for the interpretation of the P_2 apparent resistivities (Fig. 5), have to be constrained by the measured Schlumberger array resistivities (Fig. 2) which determine the resistivity of the near-surface layers. Thus, the model must have high surface resistivities at the western end of the line and very low resistivities at the eastern end. Two models which fit both the Schlumberger and P_2 apparent resistivities are shown in Figs. 5b and 5c. Both require the resistivity of the deep layer to be about 80 Rm. From the point of view of geothermal resource assessment, the important feature is the boundary between high and low resistivities (at position x ≡ -0.8 km along A'A'). This boundary is more than 1 km west of the 100 Ωm contour on the Schlumberger AB/2 = 500 m map (Fig. 2), which suggests that the Waikite-Puakohurea resistivity anomaly is more extensive than previously thought.

Line B: This line starts near the current transmitter, passes through the main part of the Waikite thermal area, then traverses the Paeroa scarp at a point where the scarp is about 135 m high. The modelling (Fig. 6) shows that the scarp causes a topographic effect, assuming a uniform earth, that lowers the apparent resistivities at the top of the scarp by about 15 %. The observed apparent resistivity at the top of the scarp (91 Ωm) is greater (not less) than the adjacent values which cannot be matched by any plausible two-dimensional model. it seems likely that there are some local inhomogeneities at the site, perhaps zones of steam, since the site is near steaming cliffs.

Again, interpretation was constrained by the requirement that the model must fit both the Schlumberger array and P_2 apparent resistivities. This led to the model shown in Fig. 6b which is similar to that obtained for Line A'A'. The

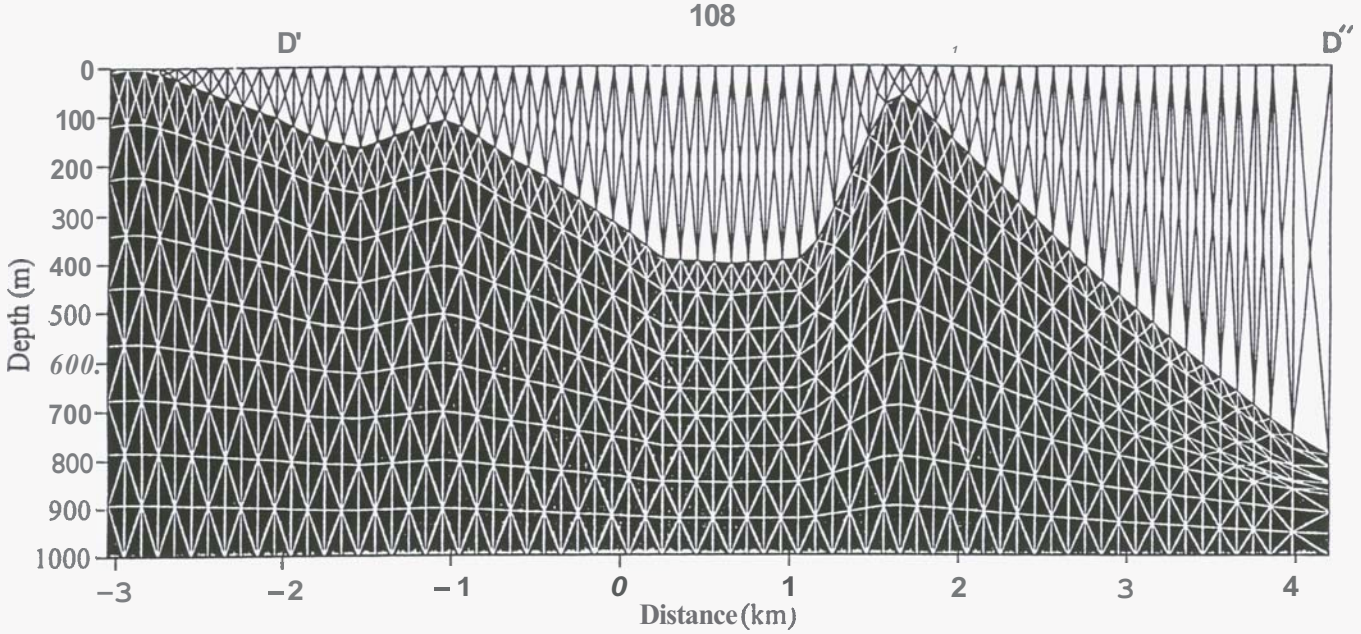

Fig. 3: Central part of the finite-element network of 6,000 elements used for the earth model in Fig. 4. The upper (unshaded) region has resistivity 100,000 Ωm, representing air; the lower half space is a uniform earth of resistivity 100 Ωm. In order to minimise the space occupied by air at the west of the fault, this particular model is inclined to the east by 7°. Beyond the edges of the figure, the element size gets progressively larger towards the outer boundaries which are at x = ±500 km, z = 400 km.

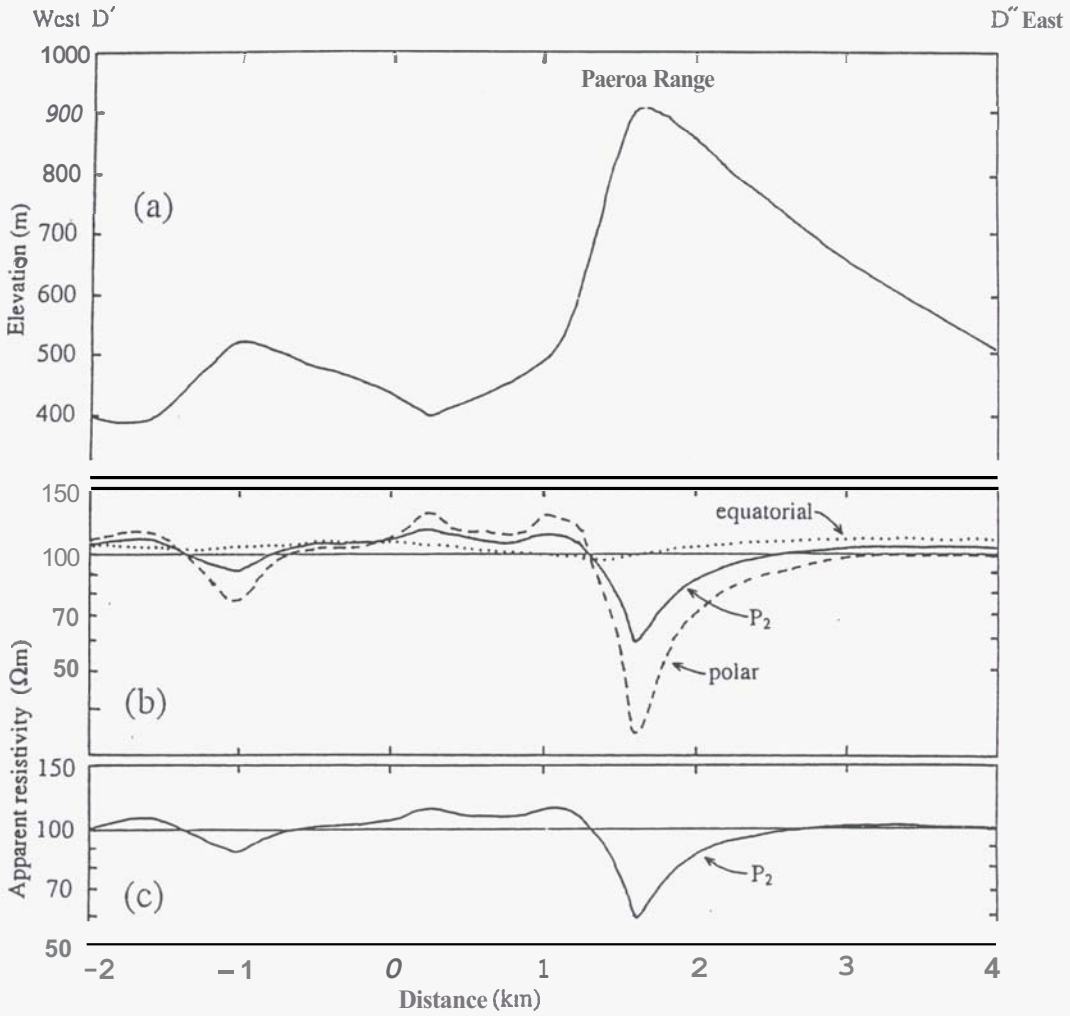

Fig. 4: (a) Topography across the Paeroa Fault on line D'D''. In (b) and (c) theoretical apparent resistivities are shown for the multiple-source bipole-dipole array set on a uniform earth of resistivity 100 Ωm. For (b), the transmitter is on the measurement line (D'D''), about 6 km to the west of the scarp. For (c), the transmitter is offset from line D'D'' by 6.9 km to the north, simulating the geometry of the array used for the field measurements.

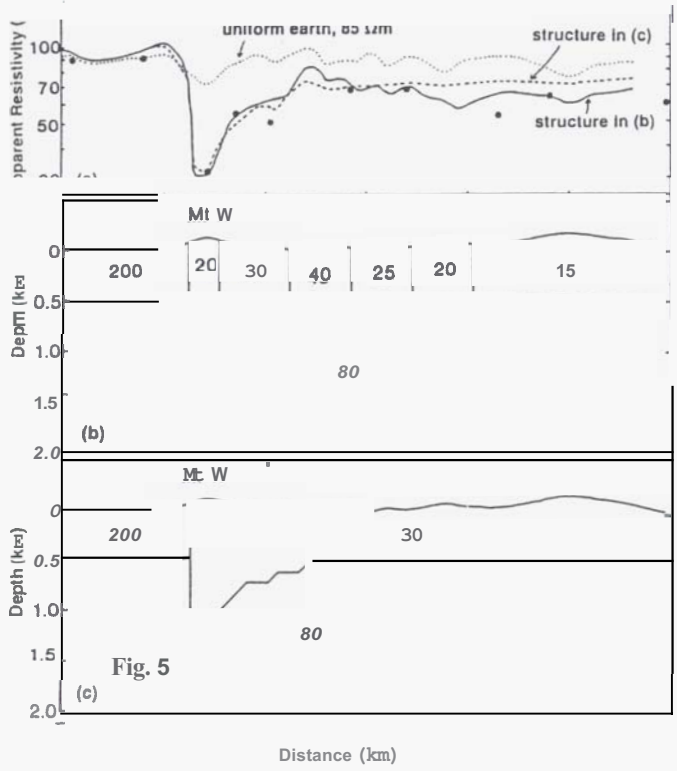

Fig. 5

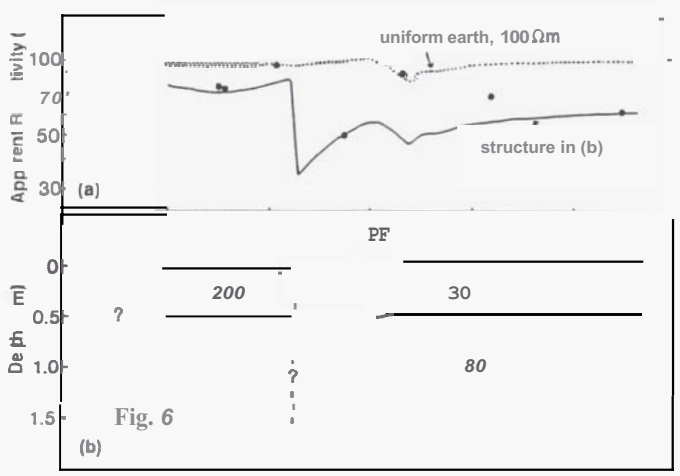

Fig. 6

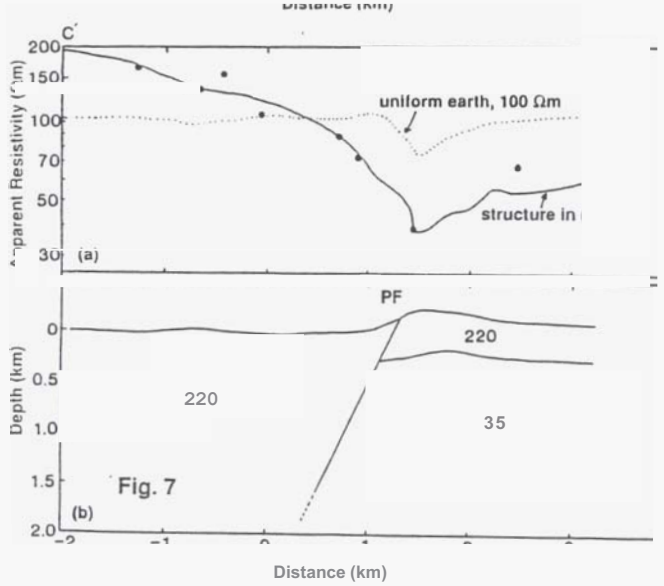

Fig. 7

spacings between P_2 measurement points to the west of Waikite was too large to accurately locate the boundary of the low-resistivity region. However, it occurs about **0.2** – 0.7 km west of the of the fault scarp, on the down-thrown side. This is in reasonable agreement with the Schlumberger data.

Lines C and D: Since the Paeroa scarp is higher on these two **lines – 250** m **on** line C'C", and **425** m on D'D" – the topographic effect on P_2 apparent resistivities is also greater. Fig. 7 shows that topography causes the P_2 values to be reduced by about **25** % on line C'C", and, as discussed above, there is **a** reduction of about **41 %** on line D'D'.

Schlumberger resistivities are high along lines CC' and D'D", except at the eastern end of line CC'. **Thus,** models similar to those on lines A'A" and **B'B"** cannot be adapted to fit. After trying many different models, the best fit for line C'C"was obtained with the model shown in Fig. 7. This model has **a** dipping resistivity discontinuity that, if extrapolated, breaches the surface at the Paeroa Scarp. It may represent the Paeroa Fault, itself. The rock resistivity is 220 Ωm both to the west of the fault and in a surface layer, **400** m thick, on the upthrown side. Below 400 m depth, on the up-thrown side, a much lower resistivity of **35** Ωm is inferred. However, **a** model with a thicker surface layer and **a** correspondingly higher deep resistivity value would fit nearly **as** well. For line D'D", further south, a model (not shown) similar to that in Fig. 7 was obtained.

The low resistivity material underlying the up-thrown Paeroa Block probably represents the old buried ignimbrites identified by Risk ***et al.*** **(1994)** under the Paeroa Block **to** the south of Waiotapu and Waikite.

In the inferred models on lines C'C" and D'D", there is no surface low-resistivity block near the Paeroa Fault that can be identified **as** a geothermal field. Thus, we infer that the Waikite thermal region has its southern limit between lines B'B' and C'C", and that the Waikite and Te Kopia fields are not connected by **a** near-surface low-resistivity zone. This is at variance with the interpretation put forward by Bromley **(1992, 1993).**

CONCLUDING REMARKS

The size of resistivity anomalies generated by two-diincnsional topographic structures can be assessed using modelling with the finite-element method. For gently sloping structures of limited extent, topographically

Figs. 5 – 7: Resistivity modelling along tines A'A", B'B" arid C'C". In part (a) of ***each*** *figure, large dots show measured apparent resistivities, dotted lines sliow modelled values for a uniform eartli. Other lines sliow resistivities for tlte models in parts (b) and (c) of tlie diagrams. On Fig. 5,* **Mt** *W indicates the ridge on Mt Waikorapa and on Figs 6 and 7* **PF** *indicates* ***the*** *scarp of tlie Paeroa Fault.*

induced anomalies in multiple-source bipole-dipole resistivity data are not much greater than the expected measurement and modelling errors, and, except for detailed investigations, can be ignored. For extreme topography, such as across the highest parts of the Paeroa Scarp, the topographic effect can become significant – along line D'D" it is about 40 %.

The modelling along lines across the Paeroa Fault shows that the topographic effect consists mainly of a low-resistivity anomaly at the crest of the scarp and a smaller high-resistivity anomaly at the base. The magnitudes of these anomalies appears to be greatest where the curvature of the surface is most extreme and they drop off quickly with distance from the scarp. This suggests that the resistivity effect of topography can be treated as a local heterogeneity, with an area of influence that is limited in extent.

Over two-dimensional structures, the topographic effect on (total field) apparent resistivity data measured with a single dipole is greatest when the current flow is perpendicular to the structure, and least (negligible) when the flow is parallel to the structure. For three dimensional structures, this distinction is no longer valid; no direction of current flow will be free of influence from the topographic effect. For correction of topographic effects from these more complex structures, tensor analysis techniques will have many advantages over the traditional total field approach.

Investigation of the low-resistivity anomalies along the Paeroa Fault with these modelling methods suggests two different causes for the anomalies. For the southern two lines, which have the highest and steepest topography, the anomalies can be accounted for by the topographic effects alone. But, on the two northern lines, which have more gentle topography and pass through the Waikite-Puakohurea thermal region, the topographic correction (only 15%) is insufficient to account for the resistivity lows Hence, these lows appear to have hydrothermal origins, associated with the local thermal region.

ACKNOWLEDGMENTS

We gratefully acknowledge assistance from D.E. Keen, S.L. Bennie, D.J. Graham and H.H. Rayner with the field-work, and from T.G. Caldwell for data analysis systems and the development of the ideas in this paper. This work was supported by Foundation of Research, Science and Technology grant C05207. This paper is Institute of Geological & Nuclear Sciences contribution 687.

REFERENCES

Bibby, H.M. (1977). The apparent resistivity tensor. *Geophysics*, 42: 1258 - 1261.

Bibby, H.M. (1986). Analysis of multiple-source bipole-dipole resistivity surveys using the apparent resistivity tensor. *Geophysics*, 51: 972 - 983.

Bibby, H.M. and Hohmann, G.W. (1993). Three-dimensional interpretation of multiple-source bipole-dipole resistivity data using the apparent resistivity tensor. *Geophys. Prosp.* 41,679-723.

Bibby, H.M., Bennie, S.L., Graham, D.J. and Rayner, H,H. (1993). Electrical resistivity map of New Zealand 1:50,000, *Sheet U16*, Institute of Geological & Nuclear Sciences, Wellington, N.Z.

Bibby, H.M., Bennie, S.L., Stagpoole, V.M. and Caldwell, T.G. (1994). Resistivity structure of the Waimangu, Waiotapu, Waikite and Reporoa geothermal areas, New Zealand. *Geothennics. 23:* 445 - 471.

Bibby, H.M., Caldwell, T.G., Davey, F.J. and Webb, T.H. (in press). Geophysical evidence on the structure of the Taupo Volcanic Zone and its hydrothermal circulation. J. *Geothenn.* and *Volcanol. Res.*

Bibby, H.M., Glover R.B. and Whiteford, P.C.. (1995). The heat output of the Waimangu, Waiotapu-Waikite and Reporoa geothermal systems: Do chloride fluxes provide an accurate measure? *Proceedings 17th N.Z. Geothermal Workshop 1995,* University of Auckland.

Bromley, C.J. (1992). Waikite - Te Kopia: the missing link? *Proceedings 14th N.Z Geothermal Workshop 1992*, University of Auckland. *14:* 217 - 222.

Bromley, C.J. (1993). Tensor *CSAMT* study of the fault zone between Waikite and Te Kopia Geothermal Fields. J. *Geomag. Geoelectr.* 45, 887-896.

Coggon, J.H. (1971). Electromagnetic and electrical modeling by the finite difference method. *Geophysics 36,* 132-135.

Fox, R.C., Hohmann, G.W., Killpack, T.J. and Rijo, L. (1980). Topographic effects in resistivity and induced-polarisation. *Geophysics,* 45: 75-93.

Glover, R.B., Klyen, L.E. and Crump, M.E. (1992). Spring' chemistry of Waikite-Puakohurea thermal area. *Proceedings 14th N.Z Geothennal Workshop 1992,* University of Auckland. *14:* 63 - 72.

Geophysics Division DSIR (1985). Electrical resistivity map of New Zealand 1:50,000, Sheet U17, DSIR, Wellington, NZ.

Grindley, G.W. (1959). Geological Map of New Zealand, 1:63360: Sheet N85 - Waiotapu. DSIR, Wellington, NZ.

Grindley, G.W., Mumme, T. C. and Kohn, B. P. (1994). Stratigraphy, paleomagnetism, geochronology and structure of silicic volcanic rocks, Waiotapu/Paeroa Range area, New Zealand. *Geothennics. 23:* 473 - 499.

Risk, G.F.; Caldwell, T.G. and Bibby, H.M. (1994). Deep resistivity surveys in the Waiotapu-Waikite-Reporoa, region, New Zealand. *Geothennics.* 23: 423 - 443.

Stewart, M.K. (1994). Groundwater contributions to Waikite geothermal fluids. *Proceedings 16th N.Z Geothermal Workshop 1994,* University of Auckland. *16:* 109 - 114.

Wood, C.P. (1994). Aspects of the geology of Waimangu, Waiotapu, Waikite and Reporoa geothermal systems, Taupo Volcanic Zone, New Zealand. *Geothermics. 23:* 401 - 421.